

UAS and a virtual environment as possible response tools to incidents involving uncontrolled release of dangerous gases – a case study

Anna Rabajczyk^{1*}, Jacek Zboina¹, Maria Zielecka², Radosław Fellner², Piotr Kaczmarzyk¹, Dariusz Pietrzela¹, Grzegorz Zawistowski¹

¹ Scientific and Research Centre for Fire Protection, National Research Institute, Nadwiślańska 213, 05-420 Józefów, Poland

² Fire University of Warsaw, Słowackiego 52/54, 01-629 Warsaw, Poland

Abstract

Various types of events and emergency situations have a significant impact on the safety of people and the environment. This especially refers to the incidents involving the emission of pollutants, such as ammonia, into the atmosphere. The article presents the concept of combining unmanned aerial vehicles with contamination plume modelling. Such a solution allows for mapping negative effects of ammonia release caused by the damage to a tank (with set parameters) during its transport as well as by the point leakage (such as unsealing in the installation). Simulation based on the ALOHA model makes it possible to indicate the direction of pollution spread and constitutes the basis for taking action. Additionally, the use of a drone allows to control contamination in real time and verify the probability of a threat occurring in a given area.

* Corresponding author, e-mail:
arabajczyk@cnbop.pl

Article info:

Received: 11 December 2023

Revised: 13 February 2024

Accepted: 29 February 2024

Keywords

unmanned aerial system (UAS), ammonia, emergency situations, ALOHA

1. INTRODUCTION

In various sources migration of natural and anthropogenic substances is more and more often presented in the form of mathematical models. These, in turn, are assumed to reflect the real world. These models enable the prediction of a chemical's concentration in different environmental components and at various times, provided that the amount of the chemical released into the environment, i.e. the pollutant's load, is known (Bessagnet et al., 2020). The behaviour and spread of a chemical in the environment depends on its physicochemical properties, the way it is introduced into the environment, and the characteristics of the environment into which it is released (National Academies of Sciences, Engineering, and Medicine, 2016). Models are used to integrate information on the multiple processes of transport and chemical transformations. They make it possible to present the behaviour and migration of a chemical compound in the environment in an accessible and transparent manner (Al Fayed et al., 2019; Batstone et al., 2015; Giompapa et al., 2007; Pirrone et al., 2010; Rasheed et al., 2019).

One of such substances is ammonia, which clearly affects air quality, contributes to environmental and climate changes, as well as poses a threat to human life and health (Van Damme et al., 2018; Zheng et al., 2015). Ammonia was included as a significant air pollutant in the Gothenburg Protocol of 1999 (United Nations, 2013) with later annexes

(UNECE, 2019). It plays a key role in the nitrogen cycle and is the main component of the total reactive nitrogen present in the atmosphere. It should be remembered that the harmful effects of ammonia on humans are mainly due to the deterioration of pulmonary function and visual disturbances (Bai et al., 2006; Bittman et al., 2015; Naseem and King, 2018). Ammonia is quickly absorbed and excreted in the upper respiratory tract, therefore, it does not cause changes in the deeper tissues of the body (Malm et al., 2013). There is no information on the teratogenic, genotoxic or carcinogenic effects of ammonia in the available literature. However, exposure to concentrations above 2,500 ppm can be fatal if the duration of exposure exceeds 30 minutes and is immediately lethal at 5,000 ppm (Neghab et al., 2018). Consequently, an increase in NH₃ emissions has a negative impact on the environment and public health, and may also affect climate change (Giannakis et al., 2019). For these reasons, it is vital to take appropriate action in the event of a risk of uncontrolled emission of this gas to the environment and to minimize the risk to entities involved in response to such a threat.

The available data show that the largest source of NH₃ emissions, accounting for over 95% of its emissions, is agriculture, including livestock farming and the use of NH₃-based fertilizers (Battye et al., 2003; Fu et al., 2020; Pan et al., 2022; Wyer et al., 2022). Other sources of NH₃ include industrial processes, vehicle emissions and volatilization from soils and oceans (Sapek, 2013; Sutton et al., 2000; Wu et al., 2016;



Wu et al., 2020; Zhan et al., 2021). Recent studies indicate that NH₃ emissions increased by 90% on a global scale over the last few decades, i.e., from 1970 to 2005 (Sommer et al., 2019). For the first decade of the 21st century, the EDGAR emissions model reports a 20% increase of the global NH₃ emissions, but with large variations at regional and national scales (Liu et al., 2022; Luo et al., 2022; Van Damme et al., 2021). An additional difficulty is the fact that ammonia is often released in less populated or border areas, where there is not a sufficient network of measuring stations.

Constantly increasing air pollution makes it extremely important to control the quality of air. Monitoring systems are commonly used for this purpose, especially in urban areas and places of social and economic importance. In the case of regions with lower population density the distribution of elements in the permanent air quality monitoring systems is less common. This is due to economic reasons, i.e. the cost of purchase and operation of such systems. Available and constituting a large potential for air quality control and monitoring is an application of unmanned aerial vehicles (UAVs) with appropriate detectors and cameras, the choice of which depends on the purpose and scope of measurements as well as the monitored pollutant. Small unmanned aerial vehicles (mini-UAVs) equipped with specialized sensors for pollution analysis provide new approaches and research opportunities in the field of air quality monitoring and identification of emission sources. They also find applications in the atmosphere research by identifying, for example, trends in climate changes (Xiang et al., 2019) or directions of processes taking place in the atmosphere (Zappa et al., 2020) or in crisis management (AIRBEAM project, 2012–2015; CAMELOT project, 2017–2021; COMPASS2020 project, 2019–2021).

The use of UAV may be particularly important for the monitoring of gaseous pollutants leakages which sources are difficult to access and at the same time strategic for international or interregional cooperation. Such incidents may have serious consequences for the environment and the population due to the possibility of movement of the pollution cloud. Even worse, they can spread to the border areas or to the territory of a neighbouring region or state. Correctly applied protective measures require the best possible knowledge of the source of pollutant emission, trajectory of contamination movement and the negative impact on the biosphere, including humans. Therefore, when it is impossible to use stationary monitoring points, in places beyond the station's reach, it may be necessary to use autonomous platforms. The use of the atmospheric dispersion model showed that two UAVs are able to provide results of a quality comparable to a stationary monitoring network (Hiemstra et al., 2011; Šmídl and Hofman, 2013; Thykier-Nielsen et al., 1999).

Application of UAVs equipped with appropriate detectors and cameras is more commonly applied nowadays. UAV use for detection of contamination, harmful gases presents new possibilities during operations and for procedures in the event of an

incident and gas release (Jońca et al., 2022; Rabajczyk et al., 2020). For example, UAVs were used to detect gas leaks and damage to the thermal insulation of tanks at the Guiana Space Center (Ferlin et al., 2019), or during the gas explosion accident and a gas pipeline fire in Murowana Goślina (GAZ SYSTEM, 2018), extinguishing forest fires and mitigating the damage caused by fires using early detection methods (Kinaneva et al., 2019), optimization of the rescue operation in the event of a fire at Notre Dame (Vidi, 2019), gas emissions in the event of volcanic eruptions (Everts and Davenport, 2016) or detection of ethanol, formaldehyde, ammonia, or hydrogen chloride in residential neighbourhoods (Burgués and Marco, 2020; Jafernik, 2019; Pobkrut et al., 2016).

The article describes the use of an UAV equipped with an ammonia sensor as well as the ALOHA (Areal Locations of Hazardous Atmospheres) modelling program. The aim of this paper is to present the concept of combining unmanned aerial vehicles with contamination plume modelling on the example of ammonia emissions in a virtual environment. This approach has been developed within a scientific and development work carried out as a part of the project entitled "Controlling an autonomous drone using goggles (monocular)" to be used by the Polish Border Guard.

In the first stage, simulations of the ammonia plume spread for two events were carried out. They aim was to determine the minimum information necessary for the proper management of the action with the use of drones and a virtual drone control system. Next, the results of simulations using the ALOHA program were implemented in scenarios of ammonia emissions from tank and from the point source formed due to unsealing created in the pipeline. Then, the results obtained were analysed in terms of the possibility of using them in the newly developed system: for selection of parameters and drone construction (including: type of sensors, weight, design) and, in the end, assessment of the usefulness of this system in case of the absence of permanent monitoring points.

2. MATERIALS AND METHODS

2.1. Simulation requirements for the ALOHA program

The computer program ALOHA (Areal Locations of Hazardous Atmospheres) was used to perform the simulation. In general, the functions included in the program can be used to model the following phenomena: release and dispersion (for low or heavy gases), influence of averaged terrain roughness, liquid fire in the tank, pool fires, jet fire and explosion (CAMEO®Software Suite, 2016).

To perform dispersion simulations, which are the subject of this study, the Gauss model was used. The formula of the Gauss model used in the ALOHA program is described by the equation (Bhattacharya and Kumar, 2015):

$$C(x, y, z) = \frac{Q}{2\pi\sigma_y\sigma_z u} \exp\left(-\frac{1}{2}\left(\frac{y}{\sigma_y}\right)^2\right) \cdot \left(\exp\left(-\frac{1}{2}\left(\frac{z-H}{\sigma_z}\right)^2\right) + \exp\left(-\frac{1}{2}\left(\frac{z+H}{\sigma_z}\right)^2\right)\right) \quad (1)$$

where:

C – pollutant concentration at a given point [g/m^3],

x, y, z – distance from source (x – downwind, y – crosswind, z – vertical),

u – the average wind speed [m/s],

H – effective emission height (sum of emitter height and plume elevation) [m],

Q – pollutant emission rate,

σ_y, σ_z – standard deviations (dispersion parameters) determined as functions of vertical turbulence states and the distance of the receptor from the emission source, estimated on the basis of the atmospheric stability class (dispersion coefficients are calculated by the ALOHA program, based on given stability class, according to the algebraic expressions developed by Briggs G.A. (Hanna et al., 1982; U.S. Department of Energy, 2004; U.S. Department of Energy, National Nuclear Security Administration, 2007).

Referring to simulation tool, it should be remembered that the program uses some simplifications during the calculations, including the lack of modelling the dispersion effects associated with the terrain obstacles, e.g., terrain unevenness (Fig. 1) (Lee et al., 2018).

ALOHA takes into account the indicated phenomena by dividing the transport equations into three emission zones with appropriately selected factors, such as the dispersion parameters. To create an appropriate emergency release scenario, the program capabilities allow to characterize the source of the threat as direct, puddle, tank and gas pipeline (Fu et al., 2020). The simulation based on the ALOHA program makes it possible to determine the time in which the substance will be released into the environment, the range of the impact of the event in the selected direction, and it takes into account the prevailing meteorological conditions. It can also estimate the concentration of the chemical substance as a function of distance and time from the leak location.

In order to determine the value of the degree of hazard in relation to toxicity, the parameter AEGL (Acute Exposure Guideline Level) is used, defined as the toxicological threshold values of the concentration of a substance directly hazardous to humans (Fig. 1) (National Academies of Sciences, Engineering, and Medicine, 2016; National Research Council, 2001; CAMEO®Software Suite, 2016).

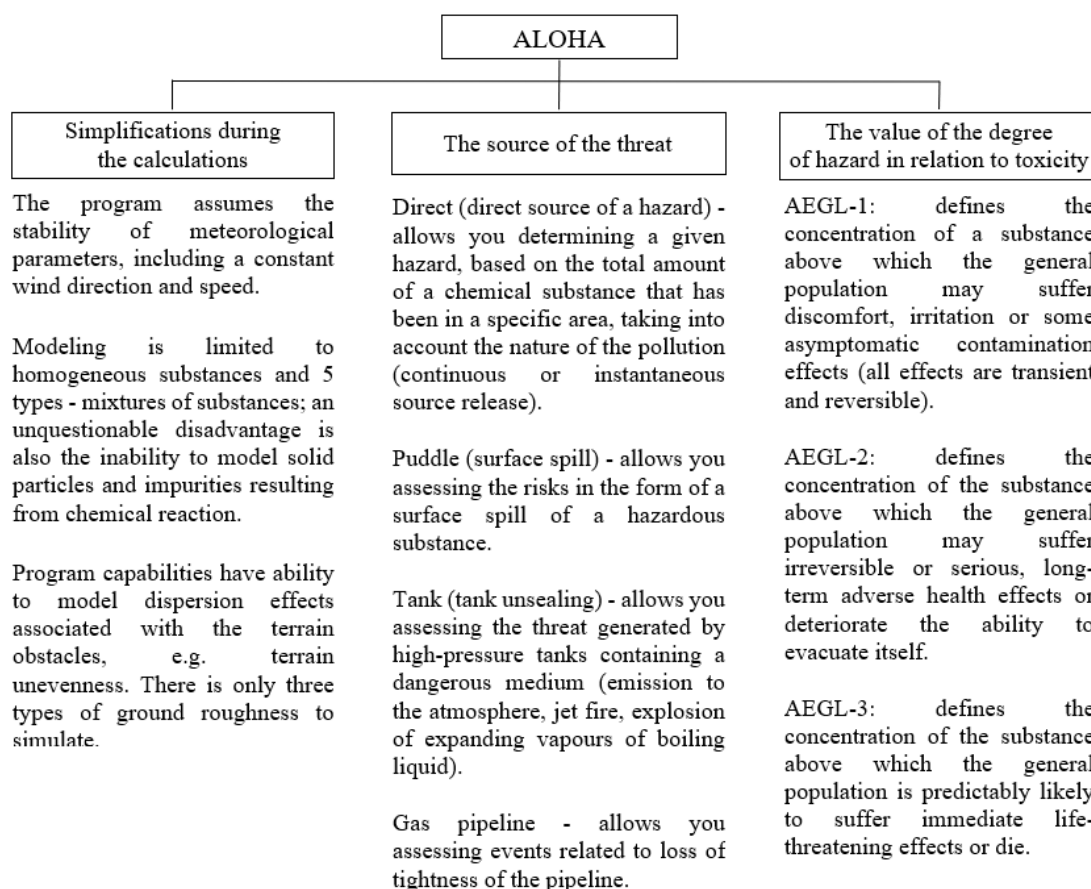


Figure 1. Characteristics of selected limitations and applications of the ALOHA program (Fu et al., 2020; Lee et al., 2018; National Research Council, 2001; CAMEO®Software Suite, 2016).

2.2. Modelling data – case study

The simulations included selected parameters reflecting real conditions, which allowed for presenting the risk of ammonia dispersion in the event of two representative situations, i.e., a tank with given characteristics (Table 1) and a leak point (Table 1) under specific conditions (Table 2). Cylindrical tanks are very often used in industrial plants and in transport. The point source simulates the emission conditions from the pipeline failure carrying the gas. The parameters (Table 2) used for the simulation correspond to the assumptions used to create emergency plans (documents developed in the event of an accident, unpredictable circumstances and sudden events and developed individually by the units responsible for security)

Table 1. Parameters used to simulate ammonia emissions for the ALOHA / RAILCAR model for all scenarios.

Parameter	Characteristic
Simulated phenomenon: Tank emission	
Medium	NH ₃
Leakage from tank	Diameter: 2.3 m Length: 13.4 m Volume: 55,674 dm ³ Filling of the tank with NH ₃ : 50%
The roughness of the substrate	Open country
Cloudy	Partly cloudy
Inversion height [m]	Without inversion
Air humidity [%]	50
Internal tank temperature [°C]	Ambient temperature
Ammonia mass – resultant [kg]	17889
Description of the release	Hole, without ignition, emissions to the atmosphere
Hole	Round, diameter 0.1 m
Physical state	50% liquid
Simulated phenomenon: Direct source of a hazard	
Medium	NH ₃
Leakage from tank	50 kg/s, duration: 30 min
The roughness of the substrate	Open country
Cloudy	Partly cloudy
Inversion height [m]	Without inversion
Air humidity [%]	50
Internal tank temperature [°C]	Ambient temperature
Ammonia mass – resultant [kg]	17,889
Physical state	50% liquid
Emission source height [m]	0; 1.15

by the State Fire Service, equipped with specialized gear designed to fight fires, natural disasters and other local threats. The simulation also takes into account criteria important for the correct conduct of the action and allows to develop a strategy for using the drone and controlling the drone based on a monocular.

The simulation parameters (Table 2) were selected to indicate different weather conditions in order to indicate the differences in emission and the displacement of the plume which correspond to summer conditions (30 °C) and winter conditions (–20 °C). Also, the height of the emission source influences changes in the emission, therefore three parameters were selected from the ground up to 50% of the tank or pipeline height.

Table 2. Variable parameters used for the simulation for both objects.

Scenario No.	Wind speed and direction [m/s]	The height of emission source [m]	Ambient temperature [°C]	Relative humidity [%]	Atmospheric stability class*
1	1	0	30	50	B
2	1	1.15	30	50	B
3	8	0	30	50	D
4	8	1.15	30	50	D
5	25	0	30	50	D
6	25	1.15	30	50	D
7	1	0	–20	5	B
8	1	1.15	–20	5	B
9	8	0	–20	5	D
10	8	1.15	–20	5	D
11	25	0	–20	5	D
12	25	1.15	–20	5	D

*B: Moderately unstable conditions; D: Neutral conditions

Wind speed and direction, from 1 to 25 m/s, were selected to present changes and dynamics of the spread of pollutants in extreme conditions. In the case of drones up to MTOM (Maximum Take-off Mass) of approx. 25 kg, a speed of 25 m/s will be too high. However, for heavier structures (above MTOM 25 kg), intended for specialized tasks (including measurements), the recommended maximum speed will be adequate.

Exposition Guideline Level for ammonia was presented in Table 3. AEGL is calculated for five relatively short periods of exposure (10 and 30 min and 1, 4, and 8 h) (Table 3), while AEGL “levels” depend on the severity of toxic effects caused by exposure, with level 1 being the lowest and level 3 being the most severe (EPA, 2024).

Table 3. Exposition Guideline Level for ammonia (National Research Council, 2010).

Exposition Level	Unit	Time				
		10 [min]	30 [min]	60 [min]	4 [hr]	8 [hr]
AEGL 1	[ppm]	30	30	30	30	30
AEGL 2	[ppm]	220	220	160	110	110
AEGL 3	[ppm]	2,700	1,600	1,100	550	390

2.3. UAV characteristics

There are several types of UAVs used to perform various types of missions and collect data using sensors: rotocopters (e.g. multicopters, helicopters), fixed-wing (e.g. aeroplanes), hybrids (e.g. VTOL – Vertical Take Off and Landing), aerostates (e.g. balloons), flapping-wing. Each of these have advantages and disadvantages verified and widely described in the literature (Gupta et al., 2013; Lambey and Prasad 2021; Mustapić et al., 2021). Among these constructions, in the authors' opinion, rotocopters should be assigned to the greatest suitability for remote measurements of air quality and pollutants. Their greatest advantage is the possibility of hovering over the point, which increases the accuracy of measurements, as well as the possibility of vertical take-off and landing without the need to provide a runway.

It is worth mentioning, that use of a UAV equipped with an appropriate RGB (Red Green Blue), night vision or thermal camera allows for monitoring or recording images, recognizing large areas (land or sea), locating suspicious people, vehicles, damaged objects without the need to send a patrol there (Bein et al., 2015). Additional support systems such as remote object detection and automatic alerting or sending notifications directly to ground patrols support the operational work of border guards and increase the efficiency of operations (Greenblatt et al., 2008). To describe this concept, the authors decided to use the hexacopter Yuneec Typhoon H520 drone equipped with an RGB camera and air pollution analyser AT-MON FL. The rationale for this choice is that type of UAV is used in scientific research projects for the Polish Border Guard, which has a built-in camera and selected sensors (Table 4). Air pollution analyser is cost-effective and easy to deploy.

The drone is one of the elements of the tool in question, the aim of which is to optimize actions in the event of a failure. Therefore, the parameters characterizing the drone must be adapted to other elements, including the parameters of the virtual environment (see Section 2.4.). The ATMON FL used is an independent mobile system for measuring gas and dust air pollutants in forced mode. It is intended to be carried by unmanned aerial vehicles (UAV – Drones), dedicated to installation on a drone. Detection time of the sensors used to measure ammonia, which is integrated with the drone, is < 30 s (Table 4).

2.4. Virtual environment

In order to better visualise the measurement data and improve making the right decisions (e.g. relating to evacuation), it will be useful to take advantage of virtual reality technology – especially in the aspect of the UAV control interface (Kamińska et al., 2019). The implemented project aims to develop and produce a prototype of an unmanned aircraft control system using the pilot's eyesight. The developed system offers such functionalities as:

- taking control of the autonomous UAV flight using goggles as well as controllers,
- ensuring the issuing of commands and control to the UAV and the camera,
- the working length of the device is not shorter than the UAV.

The prototype of these system consists following elements:

- multicopter Yuneec H520 with E90 camera,
- ground control station ST16,
- Pico Neo2 Eye VR goggles with built-in eye tracking,
- controllers,
- notebook.

The system requires two remote controls. One operates the Ground Control Station and the other controls the UAV with the help of goggles and controllers. The pilot in the goggles can see the view from the drone's camera and the map with the UAV location. The pilot can use his eyesight to give commands: moving the camera, fly to a set point, stop an ongoing mission, return to an interrupted mission, change the speed and altitude of the drone. Due to the fact that the project concerns the sphere of security and defence and was made for the needs of the Border Guard, some information, including the appearance of the interface, cannot be made public.

What is more, these system may also use virtual reality to display additional information in the goggles, for example a map of the operational area, which is shown in Fig. 2.

Taking into account the calculations and simulations presented in the previous chapter, it should be stated that it would be fully justified and advisable to overlay the simulation results on the terrain map (for instance on 3D terrain map) seen by the operator.

3. RESULTS

3.1. Results of simulation

Figures 3–14 present the simulation results for different parameters (wind speed, the height of emission source, ambient temperature, relative humidity) for two objects, i.e., the tank (a) and direct source (b).

Table 4. Characteristics of UAS and characteristics of the analyser used during the research.

Parameters	Characteristic
Yuneec Typhoon H520, RGB camera and ground control station	
Weight (with battery and RGB camera)	2 kg
Dimensions	520 × 455 × 295 mm
Flight time	28 minutes
Maximum horizontal velocity	72 km/h
Remote control	ST16S
Maximum flying altitude	500 m
Transmission distance range	1.6 km
RGB camera	E90
Camera resolution	20 megapixel
View field	DFOV 91
Remote control/ground control station	ST16S with 7" HD Touch LCD
Application to planning mission	DataPilot™ Mission Control Software System
Air pollution analyser ATMON FL	
Weight (with battery and RGB camera)	300 g
Dimensions	Ø of enclosure max 125 mm OVERALL DEVICE HEIGHT max 115 mm
Flight time	20 minutes
Transmission distance range	1.6 km
Application to present measurement	ATMON FL GRUND UNIT
Gas/pollution module	NH ₃ /ATM-FL-NH3
Reaction time	< 30 s
Accuracy	1 ppm
Measurement range	0–100 ppm
Resolution of measurement	0.01 ppm

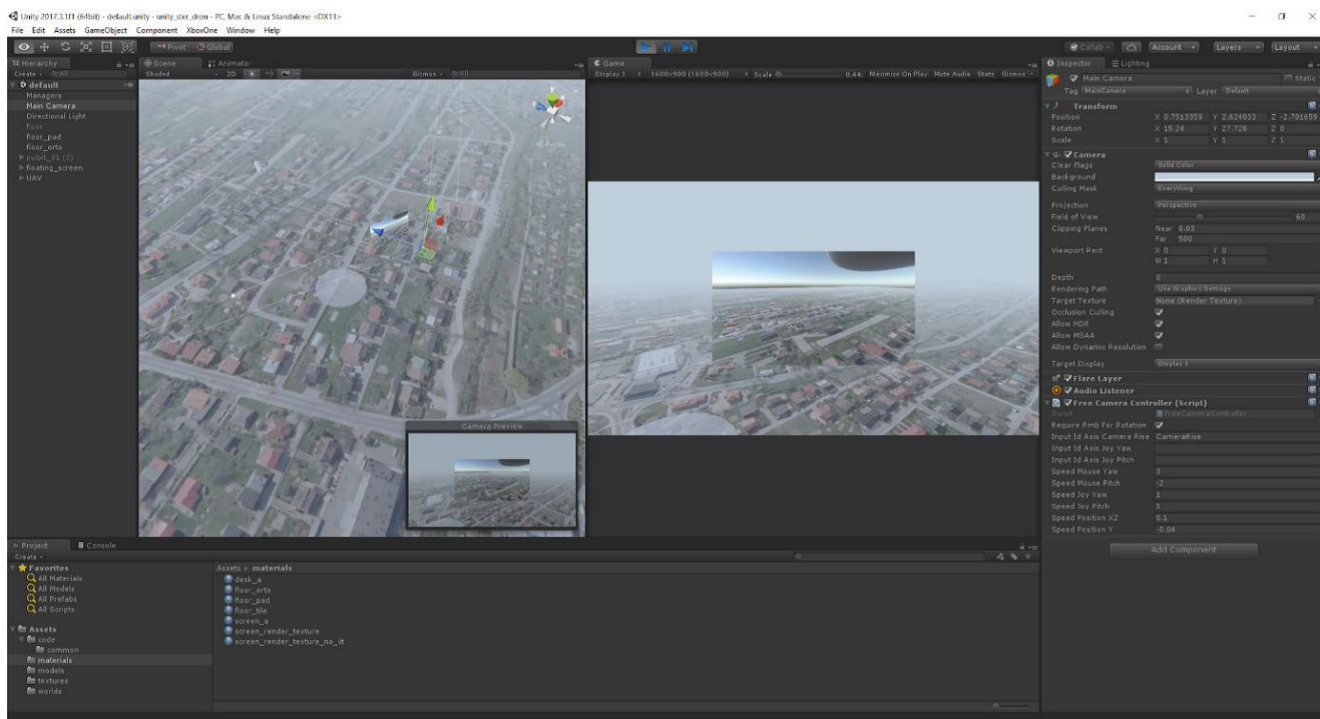
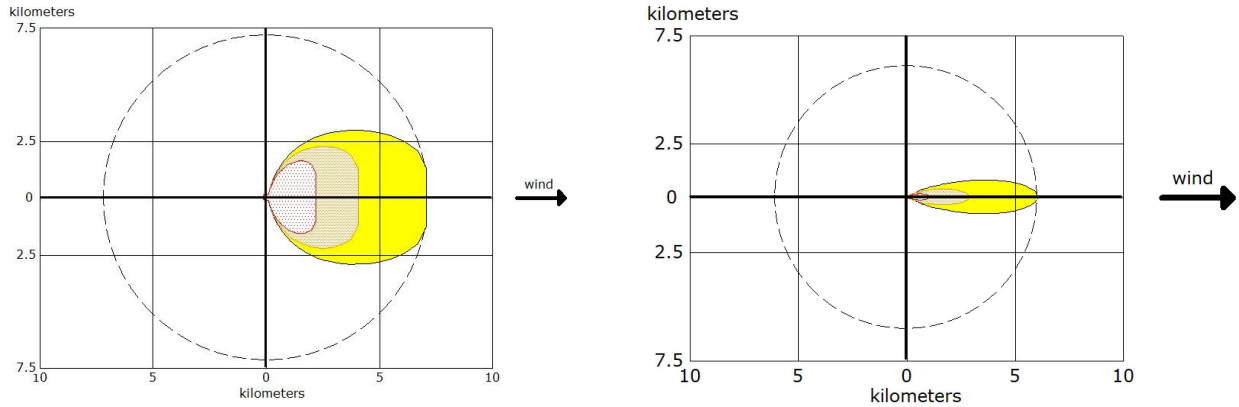
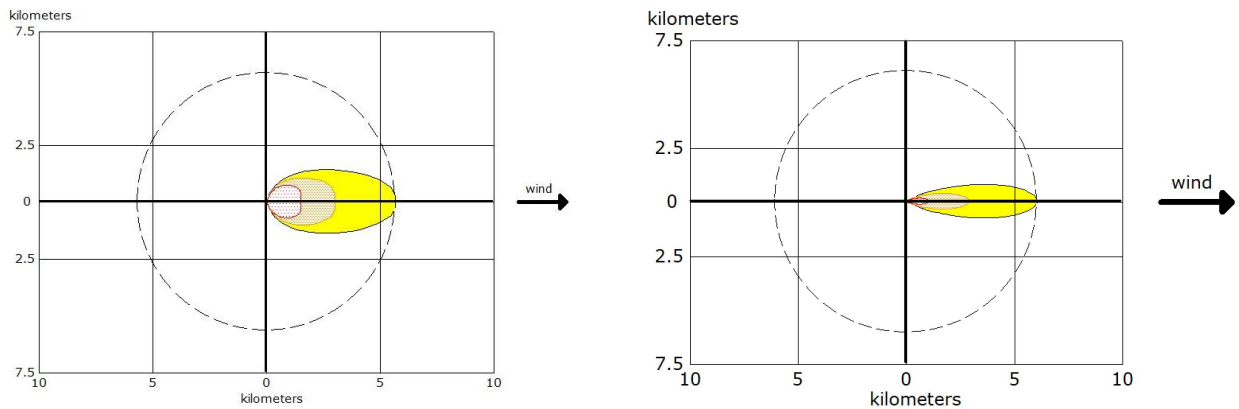


Figure 2. Screen from the prototype of the camera control system (Argasiński et al., 2019; Feltynowski 2019).



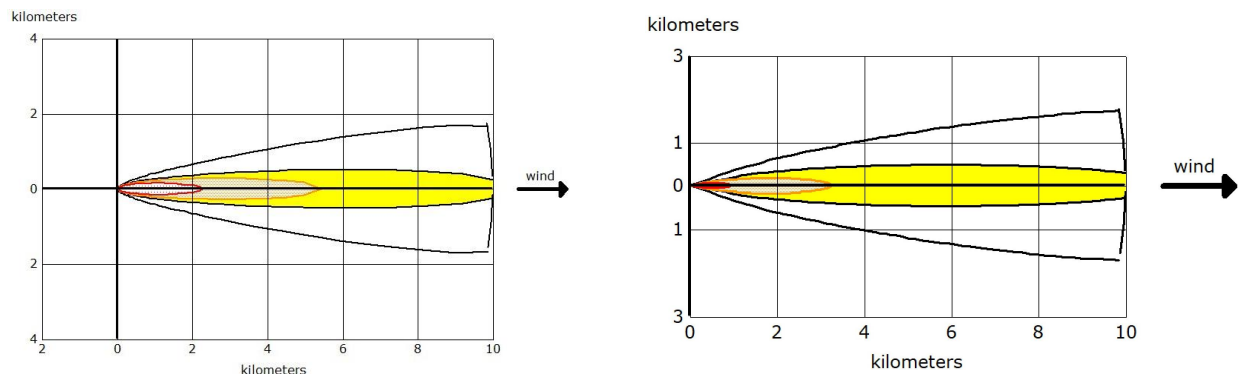
- (a) Red: 2.2 km, 1100 ppm (AEGL-3), 60 min
 Orange: 4.1 km, 160 ppm (AEGL-2), 60 min
 Yellow: 7.1 km, 30 ppm (AEGL-1), 60 min
- (b) Red: 1.0 km, 1100 ppm (AEGL-3), 60 min
 Orange: 2.8 km, 160 ppm (AEGL-2), 60 min
 Yellow: 5.9 km, 30 ppm (AEGL-1), 60 min

Figure 3. Simulation results – scenario 1 for the parameters: wind speed: 1 m/s, the height of emission source 0 m, ambient temperature 30 °C, relative humidity 50 %, atmospheric stability class B.



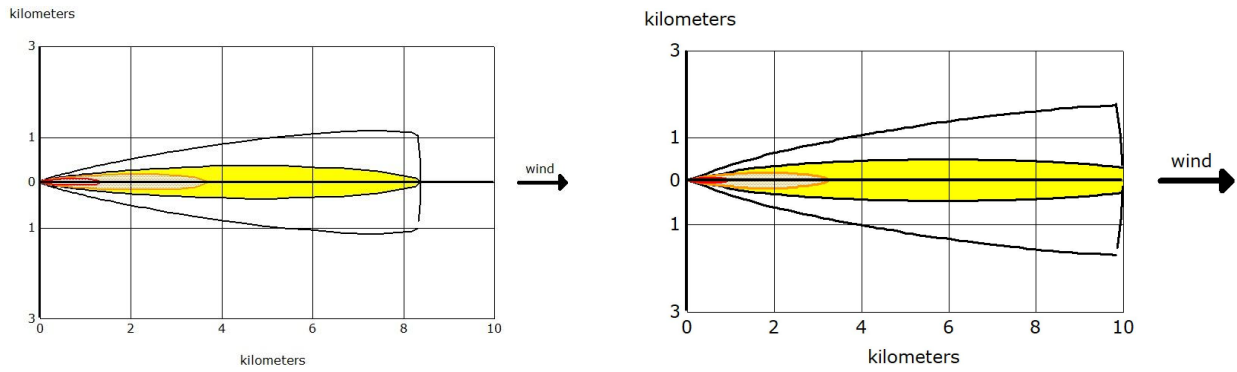
- (a) Red: 1.5 km, 1100 ppm (AEGL-3), 60 min
 Orange: 3.0 km, 160 ppm (AEGL-2), 60 min
 Yellow: 5.7 km, 30 ppm (AEGL-1), 60 min
- (b) Red: 1.0 km, 1100 ppm (AEGL-3), 60 min
 Orange: 2.8 km, 160 ppm (AEGL-2), 60 min
 Yellow: 5.9 km, 30 ppm (AEGL-1), 60 min

Figure 4. Simulation results – scenario 2 for the parameters: wind speed: 1 m/s, the height of emission source 1.15 m, ambient temperature 30 °C, relative humidity 50 %, atmospheric stability class B.



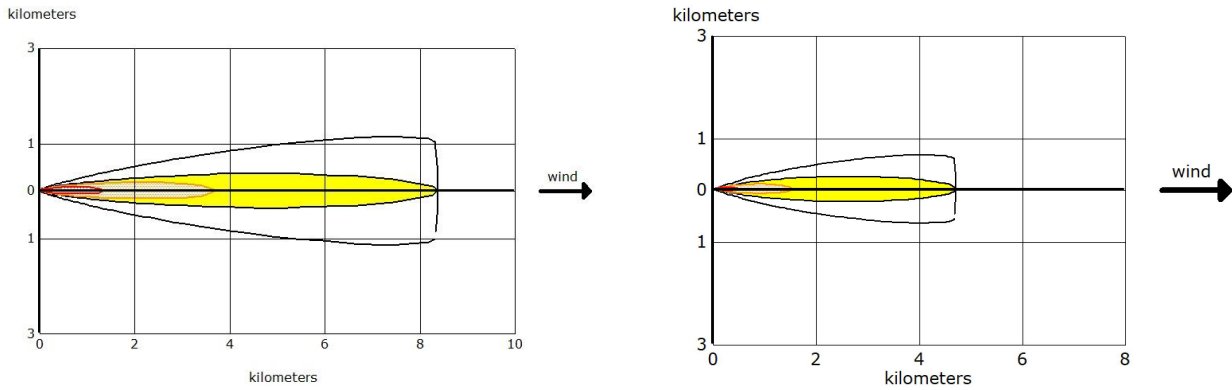
- (a) Red: 2.3 km, 1100 ppm (AEGL-3), 60 min
 Orange: 5.4 km, 160 ppm (AEGL-2), 60 min
 Yellow: greater than 10 km, 30 ppm (AEGL-1), 60 min
- (b) Red: 0,893 km, 1100 ppm (AEGL-3), 60 min
 Orange: 3.0 km, 160 ppm (AEGL-2), 60 min
 Yellow: greater than 10 km, 30 ppm (AEGL-1), 60 min

Figure 5. Simulation results – scenario 3 for the parameters: wind speed: 8 m/s, the height of emission source 0 m, ambient temperature 30 °C, relative humidity 50 %, atmospheric stability class D.



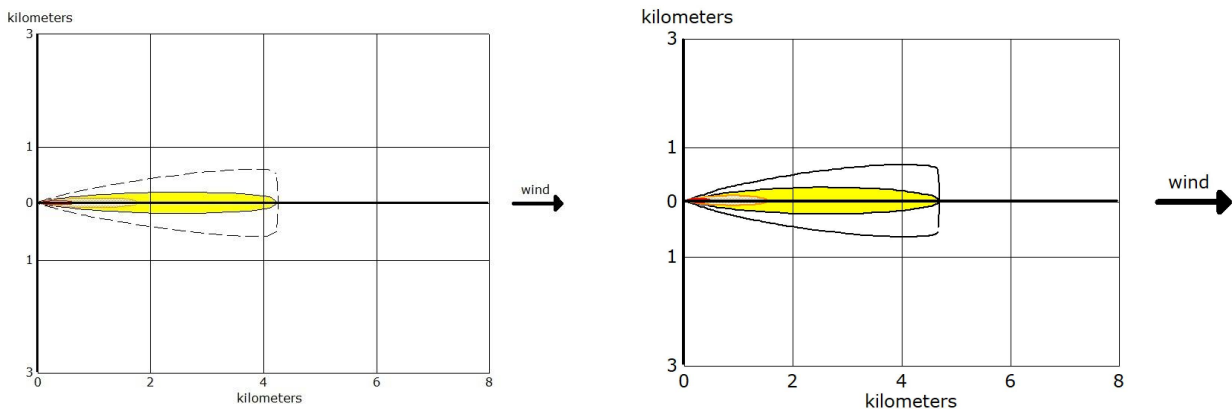
- (a) Red: 1.1 km, 1100 ppm (AEGL-3), 60 min
Orange: 3.2 km, 160 ppm (AEGL-2), 60 min
Yellow: 7.3 km, 30 ppm (AEGL-1), 60 min
- (b) Red: 0,892 km, 1100 ppm (AEGL-3), 60 min
Orange: 3.0 km, 160 ppm (AEGL-2), 60 min
Yellow: greater than 10 km, 30 ppm (AEGL-1), 60 min

Figure 6. Simulation results – scenario 4 for the parameters: wind speed: 8 m/s, the height of emission source 1,15 m, ambient temperature 30 °C, relative humidity 50 %, atmospheric stability class D.



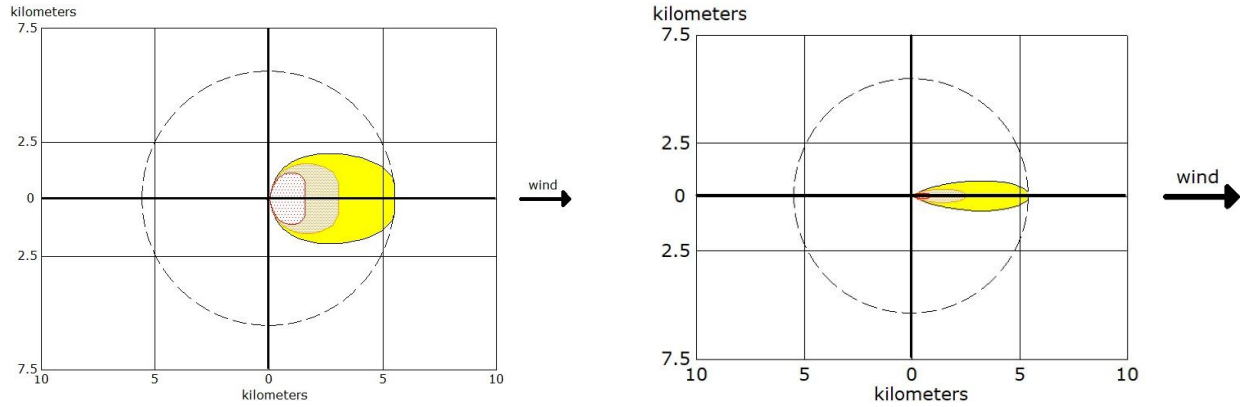
- (a) Red: 1.4 km, 1100 ppm (AEGL-3), 60 min
Orange: 3.7 km, 160 ppm (AEGL-2), 60 min
Yellow: 8.4 km, 30 ppm (AEGL-1), 60 min
- (b) Red: 0,461 km, 1100 ppm (AEGL-3), 60 min
Orange: 1.4 km, 160 ppm (AEGL-2), 60 min
Yellow: 4.4 km, 30 ppm (AEGL-1), 60 min

Figure 7. Simulation results – scenario 5 for the parameters: wind speed: 25 m/s, the height of emission source 0 m, ambient temperature 30 °C, relative humidity 50 %, atmospheric stability class D.



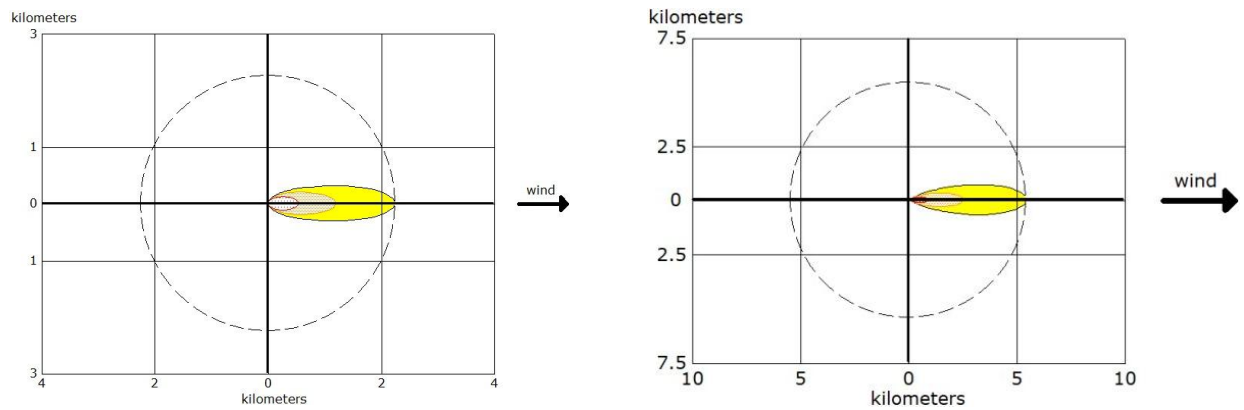
- (a) Red: 0,639 km, 1100 ppm (AEGL-3), 60 min
Orange: 1.8 km, 160 ppm (AEGL-2), 60 min
Yellow: 4.3 km, 30 ppm (AEGL-1), 60 min
- (b) Red: 0,460 km, 1100 ppm (AEGL-3), 60 min
Orange: 1.4 km, 160 ppm (AEGL-2), 60 min
Yellow: 4.4 km, 30 ppm (AEGL-1), 60 min

Figure 8. Simulation results – scenario 6 for the parameters: wind speed: 25 m/s, the height of emission source 1.15 m, ambient temperature 30 °C, relative humidity 50 %, atmospheric stability class D.



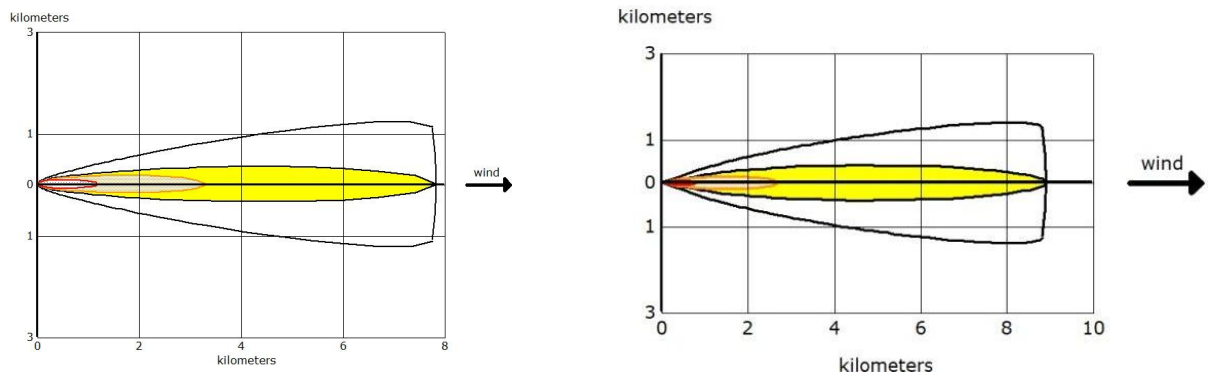
- (a) Red: 1.6 km, 1100 ppm (AEGL-3), 60 min
 Orange: 3.1 km, 160 ppm (AEGL-2), 60 min
 Yellow: 5.6 km, 30 ppm (AEGL-1), 60 min
- (b) Red: 0,934 km, 1100 ppm (AEGL-3), 60 min
 Orange: 2.5 km, 160 ppm (AEGL-2), 60 min
 Yellow: 5.5 km, 30 ppm (AEGL-1), 60 min

Figure 9. Simulation results – scenario 7 for the parameters: wind speed: 1 m/s, the height of emission source 0 m, ambient temperature -20°C , relative humidity 5 %, atmospheric stability class B.



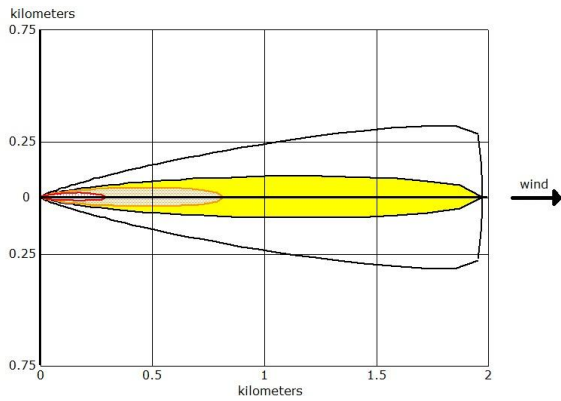
- (a) Red: 0,539 km, 1100 ppm (AEGL-3), 60 min
 Orange: 1.2 km, 160 ppm (AEGL-2), 60 min
 Yellow: 2.3 km, 30 ppm (AEGL-1), 60 min
- (b) Red: 0,934 km, 1100 ppm (AEGL-3), 60 min
 Orange: 2.5 km, 160 ppm (AEGL-2), 60 min
 Yellow: 5.5 km, 30 ppm (AEGL-1), 60 min

Figure 10. Simulation results – scenario 8 for the parameters: wind speed: 1 m/s, the height of emission source 1,15 m, ambient temperature -20°C , relative humidity 5 %, atmospheric stability class B.

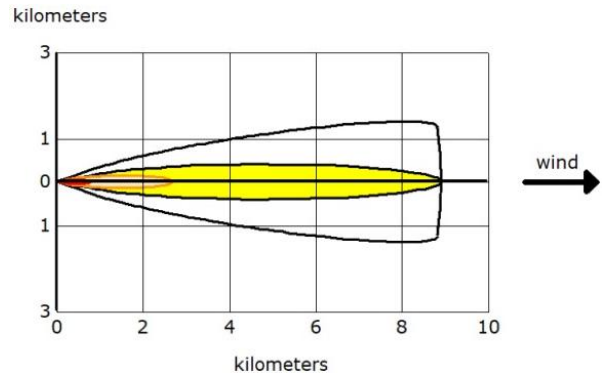


- (a) Red: 1.2 km, 1100 ppm (AEGL-3), 60 min
 Orange: 3.3 km, 160 ppm (AEGL-2), 60 min
 Yellow: 7.8 km, 30 ppm (AEGL-1), 60 min
- (b) Red: 0,802 km, 1100 ppm (AEGL-3), 60 min
 Orange: 2.7 km, 160 ppm (AEGL-2), 60 min
 Yellow: 8.9 km, 30 ppm (AEGL-1), 60 min

Figure 11. Simulation results – scenario 9 for the parameters: wind speed: 8 m/s, the height of emission source 0 m, ambient temperature -20°C , relative humidity 5 %, atmospheric stability class D.

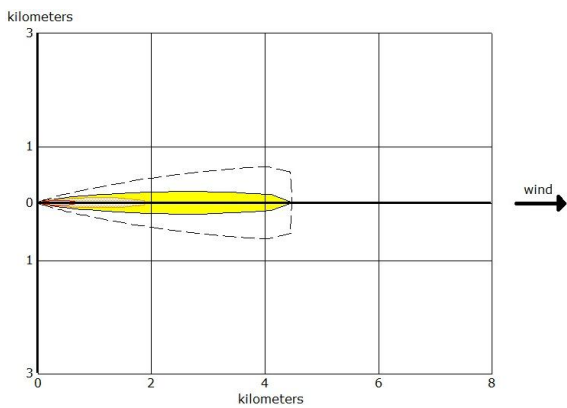


(a) Red: 0,295 km, 1100 ppm (AEGL-3), 60 min
Orange: 0,819 km, 160 ppm (AEGL-2), 60 min
Yellow: 2.0 km, 30 ppm (AEGL-1), 60 min

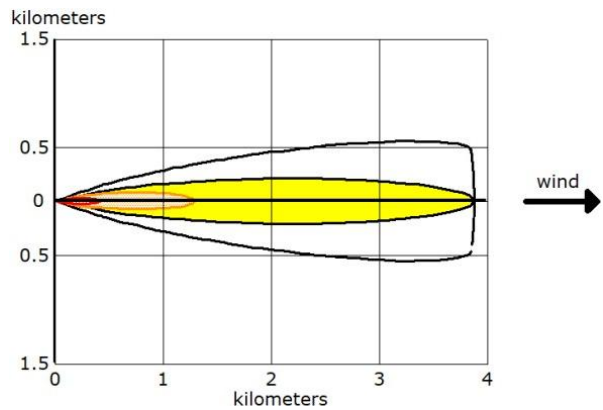


(b) Red: 0,802 km, 1100 ppm (AEGL-3), 60 min
Orange: 2.7 km, 160 ppm (AEGL-2), 60 min
Yellow: 8.9 km, 30 ppm (AEGL-1), 60 min

Figure 12. Simulation results – scenario 10 for the parameters: wind speed: 8 m/s, the height of emission source 1,15 m, ambient temperature -20°C , relative humidity 5 %, atmospheric stability class D.

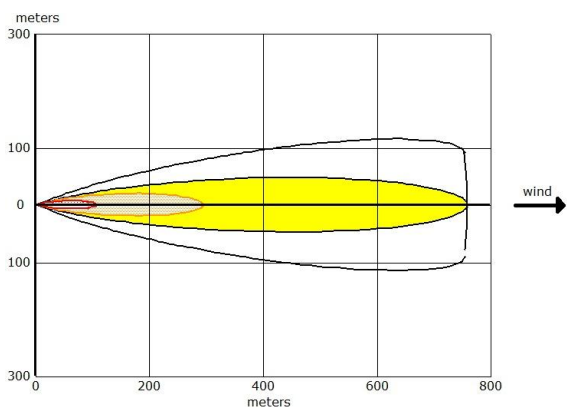


(a) Red: 0,684 km, 1100 ppm (AEGL-3), 60 min
Orange: 1.9 km, 160 ppm (AEGL-2), 60 min
Yellow: 4.5 km, 30 ppm (AEGL-1), 60 min

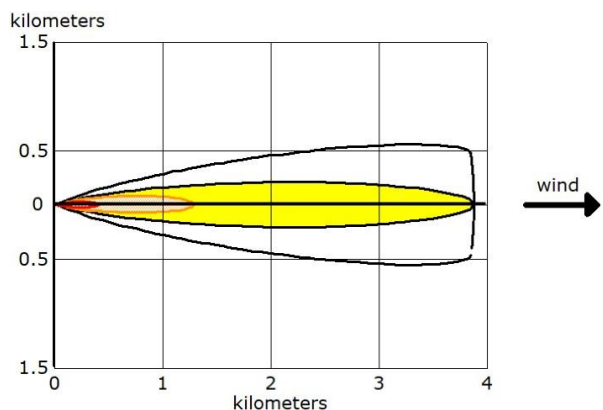


(b) Red: 0, 417 km, 1100 ppm (AEGL-3), 60 min
Orange: 1.3 km, 160 ppm (AEGL-2), 60 min
Yellow: 3.9 km, 30 ppm (AEGL-1), 60 min

Figure 13. Simulation results – scenario 11 for the parameters: wind speed: 25 m/s, the height of emission source 0 m, ambient temperature -20°C , relative humidity 5 %, atmospheric stability class D.



(a) Red: 0,106 km, 1100 ppm (AEGL-3), 60 min
Orange: 0,294 km, 160 ppm (AEGL-2), 60 min
Yellow: 0,760 km, 30 ppm (AEGL-1), 60 min



(b) Red: 0,416 km, 1100 ppm (AEGL-3), 60 min
Orange: 1.3 km, 160 ppm (AEGL-2), 60 min
Yellow: 3.9 km, 30 ppm (AEGL-1), 60 min

Figure 14. Simulation results – scenario 12 for the parameters: wind speed: 25 m/s, the height of emission source 1,15 m, ambient temperature -20°C , relative humidity 5 %, atmospheric stability class D.

4. DISCUSSION

4.1. ALOHA simulation

The ALOHA program allowed for the analysis of the migration trajectory of the toxic gas ammonia for two selected cases, including emissions from a tank of given dimensions (diameter 2.3 m, length 13.4 m, capacity 55,674 dm³) filled with 50% NH₃. The simulation of emissions from a tank that has become unsealed, e.g., during transport, takes into account the height of the emission source, the rate of ammonia release and changes in the gas content in the tank, and the range of impact. The simulations included 12 different scenarios in which the variable parameters were: wind speed, emission source height, ambient temperature, relative humidity and the atmosphere stability class (Table 2). In the case of temperature, the analysis covered two extreme cases, i.e., summertime with a temperature of 30 °C and winter time with a temperature of -20 °C. It should be added that the choice of temperature is important not only for the simulation process, but also for the selection of sensors used for the analysis. The sensors used to analyse ammonia concentration must operate in a given temperature range. It is important that measurement accuracy is maintained, acceptable to the operator. Appropriate sensor response time and sending information about the analyte concentration are also necessary. The analyser selected by the authors had a time of less than 30 s which allowed obtaining information in real time.

Ammonia is stored in a liquid state under pressure. Any time the ammonia container is opened, it may leak. The performed calculations allowed to determine the extent of the toxic cloud with a concentration above the threshold value and the direction of its movement (Figs. 3–14). Based on the data entered into the program and the adopted assumptions (Tables 1 and 2), the analysis of the effects resulting from the release of NH₃ into the environment was performed. In the first scenario (Fig. 3), the highest concentration of 1100 ppm and corresponding to AEGL-3 is within 2 km from the source, the lower than 160 ppm (AEGL-2) at 3.7 km and the lowest concentration equal to 30 ppm (AEGL-1) at a distance of 6.5 km. The distribution of pollutants was obtained for a summer day characterised by relative humidity at the level of 50 %, wind speed of 1 [m/s], atmosphere stability class B and emission at the height of 0 [m] (Fig. 3). In the case of a winter day with a temperature of -20 °C (Fig. 9), the scope of the cloud's influence is smaller and amounts to 1.6, 3.1 and 5.6 km, respectively. People in the AEGL-1 zone (Fig. 1; Table 3) are exposed to ammonia concentrations above which predictably general population may experience discomfort, irritation or some asymptomatic contamination effects. All of these effects are transient and reversible, but for those with weaker condition can lead to serious consequences. In the AEGL-2 zone, which is characterized by an NH₃ concentration above which the general population may not only experience irreversible or severe long-term adverse health effects, but also the ability to

evacuate by itself may be deteriorated. The presence of people in the AEGL-3 zone may pose an immediate threat to life or death. It should be noted that the individual sensitivity of people and the value of the standard adopted in the European Union, the TLV (threshold limit value) value of ammonia, as a weighted average value for an 8-hour working day, was set at 19.74 ppm (14 mg/m³), and the TLV-STEL (threshold limit value – short term exposure limit) value at the level of 39.48 ppm (28 mg/m³) (Neghab et al., 2018). The maximum dose to which each person within 100 m of the place where NH₃ is released from the tank during the first hour is exposed is 10 kg/min at 30 °C and 3 kg/min at -20 °C (Figs. 3, 9).

Selecting the Source Strength option in the ALOHA program gives the possibility to present the amount of a chemical substance that is released from the tank as a function of time, i.e., the determination of the "source's firepower". Information in this regard is important for people staying at the place of the leak. The obtained results allowed to determine the accuracy with which it is necessary to transmit information from the drone to the centre in order to verify changes in the pollution stream due to e.g. changes in wind speed. In the case of the simulation for the same temperature (i.e. 30 °C, Figs. 3–8, or -20 °C, Figs. 9–14), it was shown that the measurement accuracy of the height of the substance emission point cannot be less than 1 m. Lack of accuracy in this range significantly affects the assessment of both the ammonia release rate and the size of the streak. If the emission occurs at a height of 1.15 m, the impact range is smaller, while the change in wind speed is not that significant. The use of a drone allows for direct verification of data in real time. Information about the analysed parameters is transferred from the drone to the management point on an ongoing basis (the response time of the analyser is less than 30 s), which allows to update the simulation of the spread of pollution and take action in the area which becomes contaminated. The use of a monocular (Figs. 2, 19) allows to control the drone while ensuring the safety of the drone operator. Comparing the obtained simulation results for the emission situation from the 0 m point and for the 1.15 m point (Figs. 3–14), it can be noticed that the wind speed and the stability of the atmosphere are of great importance in the event of a crisis situation such as unsealing of the tanker during transport. It requires appropriate and quick action of the services.

With regard to emissions from a fixed point (e.g. from the pipeline), the results obtained indicate a significant influence of parameters such as wind speed and temperature on air pollution, as well as the amount of pollutants emitted, humidity and the atmosphere stability class. Comparing the results obtained for the same atmospheric conditions, but with a different heights of the emission point, it can be seen that the emission source height is not as a critical parameter as in the case of emissions from the tank. The change of height under the same weather conditions gives the same range of impact of ammonia. This is a consequence of the assumptions and processes included in the ALOHA. It should also be noted

that the form in which ammonia will be transported through a pipeline or in a tank also determines the processes it will undergo immediately after release.

Analysing the influence of temperature on the spread of the ammonia cloud, it can be noticed that the temperature also does not play a significant role in the analysis. Both at 30 °C and –20 °C, comparable results of the spread of the released pollutant were obtained. It should be noted, however, that in the case of the scenarios analysed for the winter period, it was noted that the impact range is slightly smaller than for the summer period. This is, of course, related to the reflection of the spread of gases depending on temperature and humidity.

The analysis of the results obtained shows that, depending on the type of failure, it is necessary to take into account the appropriate variables that affect the accuracy and safety of firefighters and other participants in the action (Fig. 15).

The results obtained correlate well with the literature data showing that the models developed as a result of simulations in the ALOHA environment are a very good support for the process of managing the risk of high hazards related to the release of dangerous gases into the atmosphere. They facilitate the selection of the optimal solution for a given event (Jones et al., 2013). For example, a simulation of the release of chlorine, epichlorohydrin and phosgene from storage tanks located at three factories in a chemical complex in central Taiwan was performed to obtain the results necessary to develop the scenarios according to the emergency response planning guidelines (ERPG) and their corresponding values directly dangerous to life or health (IDLH – dangerous to life or health) (Tseng et al., 2012). The simulations took into account the wind speed, the level of atmospheric stability and the total release time. The simulation results were used as a basis for gas leak analysis and risk assessment.

The ALOHA environment was also used to simulate failures in order to prepare crisis management scenarios. For example, Orozco et al. (2019) obtained a model of the quantitative impact on humans and the environment in the event of ammonia release from tanks in the Matanzas industrial area, Cuba

(Orozco et al., 2019). Thanks to the use of ALOHA software, various scenarios were obtained: “Toxic vapour cloud”, “Flammable area” and “Vapour cloud explosion”, and the number of victims was determined in the event of each scenario occurring. Also Nandu and Soman (2018) performed a hypothetical release of liquid ammonia from a chemical plant warehouse based on CFD (Computational Fluid Dynamics) analysis, and the dispersion of ammonia vapour in the atmosphere using ALOHA (Nandu and Soman, 2018). The results obtained by James (2015) indicate that as the wind speed increases, the danger zone decreases, because as the wind speed decreases, the period of formation of vapour clouds lengthens and the density of ammonia vapours in the atmosphere increases. The maximum risk zone calculated as a result of the simulation was obtained for a wind speed of 4 m/s. Ammonia concentrations were higher than its MRL of 25 ppm for distances of up to 5 km at a wind speed of 4 m/s. One of the main hazards in petrochemical plants is ammonia leakage. Based on the results of the HAZOP (hazard and operability) study, ammonia emissions were modelled at the petrochemical plant in Asaluyeh (Iran) (Abbaslou and Karimi, 2019). The three most likely accident scenarios were selected, including a toxic vapour cloud, a jet fire and a boiling liquid vapour expanding explosion (BLEVE). Then, scenario modelling was performed using the ALOHA environment. The toxic vapour cloud scenario assumes the release of 81,316 kg of ammonia. The concentration of toxic ammonia fumes exceeded 1,100 ppm at a distance of 1 km, causing death within 60 seconds. Overpressure never exceeds 3.5 psi; so it shall not cause serious injuries or damage to buildings. In the third scenario, BLEVE’s thermal radiation exceeded 10 kW/m² at an altitude of 376 m and could cause death within 60 seconds (Abbaslou and Karimi, 2019).

In the case of the ammonia release analysis presented in the article, conducting a simulation in the initial phase of the threat using the ALOHA model would not only be useful for the rescue commander, but also beneficial for the residents of the affected areas by letting them know about necessary precautions to ensure the safety of their lives and property.

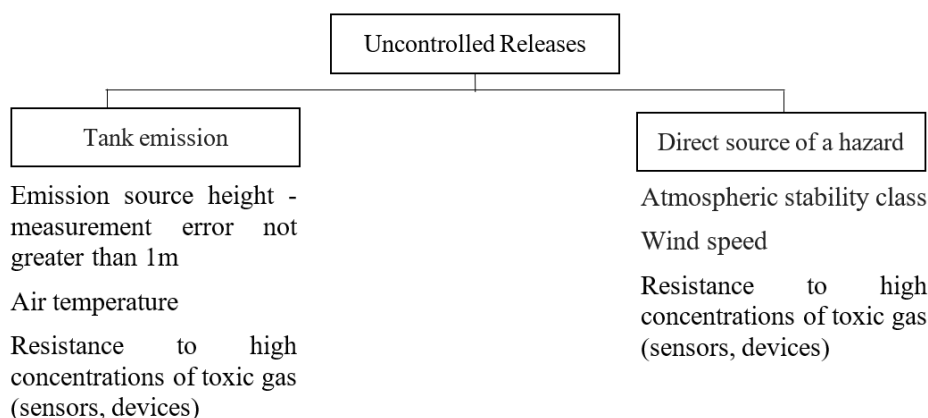


Figure 15. Selection of parameters depending on the type of event.

The use of the ALOHA model, as indicated by the results of the authors and other researchers, is a good and simple tool that allows for proper management in case of contamination threat. It can, therefore, be used as a support tool in activities aimed at protecting human health and environmental protection against hazardous gases, such as ammonia. However, it should be noted that each case must be considered individually, e.g., due to different atmospheric conditions analysed or the characteristics of the container from which the release takes place.

4.2. The use of drones and virtual reality

Comparing the obtained results for both systems, it should be stated that in the event of an accident, such as emission of the harmful substance from the tank during transport (e.g. ammonia) each element included in the ALOHA program is important and determines the formation of a cloud. Taking into account the fact that in such situations it is very often impossible to directly analyse the release rate, the temporary change in the concentration of ammonia in the air and its spread in the environment, the use of simulation methods in combination with drones is an indispensable tool for quicker threat assessment. Using the simulation results, with the assumed parameters of the atmosphere and the emission source, we obtain information about the possible path of pollution migration. The person managing the rescue operation, in the situation of gas release, through drones has the ability to track the streak and make appropriate changes to the program in order to obtain the cloud that best corresponds to the real changes taking place in the environment. It is very important that the tool is easy to apply and interpret, without high hardware requirements, and can be used in the field. The ALOHA program belongs to this type of programs. The data

obtained from the simulation allows then the UAV to be sent for verification and ongoing monitoring of the moving plume in the air. The drone, thanks to the installed appropriate sensors (Rabajczyk et al., 2020), enables the qualitative and quantitative measurement of selected air pollution.

In order to properly implement actions in the event of failure and release of hazardous gas, it was assumed to use an unmanned aerial vehicle (with an appropriate measuring system) in accordance with the following concept:

1. fly over the cloud of substances,
2. make the quantitative-quality measurement of pollution from the cloud of gas,
3. locate a place of the (unsealing, gaps, holes), assess its size,
4. send data from the measurement and size of the leak to the simulation,
5. make a simulation based on the data provided by the drone.

In order to illustrate the advantages of simulation, scenarios no 1. was selected for the analysis of tank failure cases. Next, a compilation of the simulation results from ALOHA on a map of sparsely populated area was made (Fig. 16).

As shown in Figure 16 above, the authors have obtained a picture of specific areas exposed to the result of leaks. Thus, it is now possible to plan the optimal route for the UAV coverage path. Knowing the size and shape of area affected by leakage, it will also be possible to calculate how many batteries in UAV will be needed to complete the entire mission, and how long it will take. The limitation of performed simulations is that they do not include the estimated height of the leakages. Thus, the pilot has to decide from what height a measurement should be started.

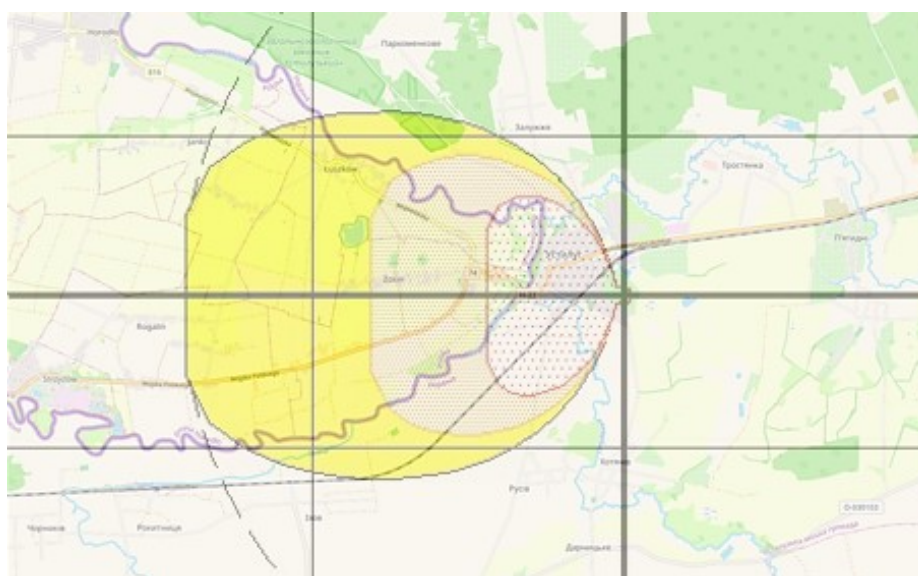


Figure 16. Compilation of results of simulation scenario no 1. and map of sparsely populated area (correct scale or proportions are maintained).

As mentioned, a simulation of a specific areas exposed to the result of a leak was obtained. It allows to arrange the appropriate shape of the flight route and plan the mission. The below figure (Fig. 17) presents the proposed flight path for simulation scenario no 1. The flight altitude was assumed to be 100 m. The planned mission shows that total time of mission is 4 hours and 38 minutes. What is more, to complete the flight up to 15 batteries are required.

The next figure (Fig. 18) presents the proposed flight path for simulation scenario no 12. The flight altitude was assumed to be 40 m, because the height of buildings is lower than in scenario no.1. The planned mission shows that total time of mission is 2 hours and 06 minutes. What is more, to complete the flight up to 7 batteries are required.

The above simulations give grounds for the statement that total time of mission is relatively long. It seems that such long-term measurement is not conducive to quick response and planning of rescue and crisis management actions. Thus, it is recommended to establish shorter path, to divide the area into smaller sectors and use several independent drones controlled by pilots at the same time. However, due to the analyser ATMON FL, the use of a drone swarm is preferred.

It should be noted that in this simulation, atmospheric conditions were not taken into account, because DataPilot™ Mission Control Software System does not have such features and does not take into account, e.g., the wind speed, humidity, air temperature when calculating the required batteries. Moreover, the maximum distance for telemetry exceeds the range of the

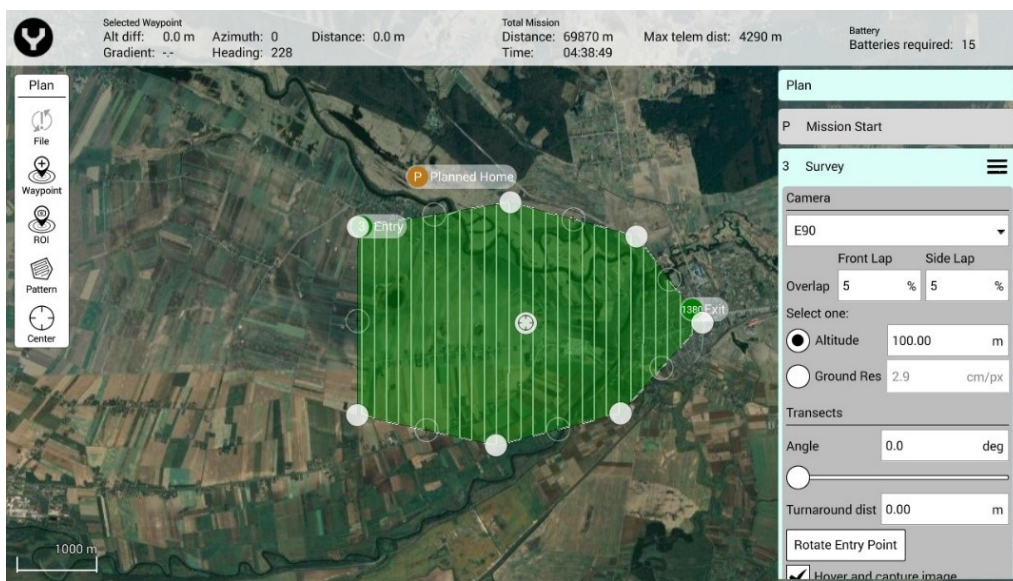


Figure 17. Proposed flight path for simulation scenario no 1. Source: DataPilot™ Mission Control Software System

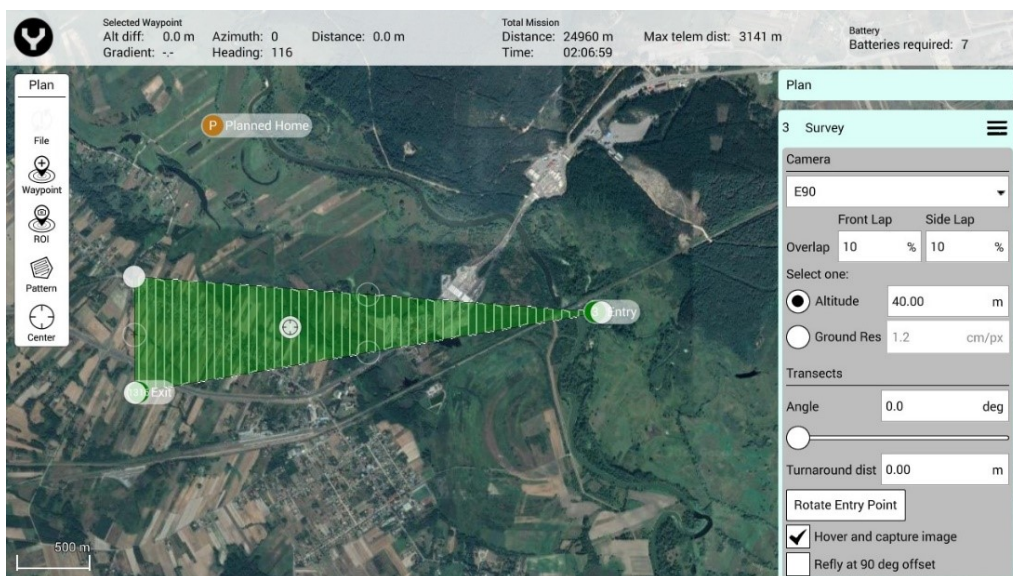


Figure 18. Proposed flight path for simulation scenario no. 12. Source: DataPilot™ Mission Control Software System

ground control station ST16S as well as air pollution analyser ATMON FL, so the pilot should have to follow the UAV in order to maintain connection and not to lose radio link.

Simulation results obtained from the ALOHA program also indicate that it is important for the operator's safety to select the analyzer appropriately to the prevailing weather conditions. If the range is too small, the operator may be exposed to contamination.

The system has been thoroughly tested to adapt its functionalities and capabilities to the needs and requirements of users (firefighters, border guards, rescue services). A prototype of such a system was tested by the project team from July till August 2021. Tests of the system are shown in Fig. 19.



(a)



(b)

Figure 19. Photos from tests in 2021 (Authors: Zawistowski and Kęty (a); Florek and Duchnow (b)).

Therefore, combining drone operation with predictions of pollution migration from modelling showed limitation and challenges using UAV and demonstrated what parameters may be important for such application (for example: UAV wind resistance, data transmission range, possibility of using the vehicle with a docking station). The combination of both tools, i.e., a drone guided by a pilot using his eyes, and the ALOHA program, allows for proper management of the drone, taking action in the contaminated area, and adapting work in the event of a change in weather conditions.

The pilot should also be aware of the uncertainties resulting from the simulation, as this will allow him to plan the mission parameters so as to properly scan the area, e.g., knowing the direction of movement, knows where the UAV should fly and in which area (surface) to check concentrations at different heights in order to detect contamination. It should be added that the uncertainty is related to the accuracy of the input data used for the simulation. The change in weather conditions determines the accuracy of the simulation. Therefore, the use of a drone and real-time data verification allows for the reduction of simulation uncertainty and allows to obtain reliable information necessary for the proper conduct of the action and react to changes occurring in real time.

The development of the concept itself showed that thanks to the performed simulations based on the assumed parameters (ALOHA), at the stage of planning it was found that technical (planned route, range of data transmission) and logistical (follow the UAV not to lose radio link) issues must be solved. The UAV flight route planning should take into account weather conditions (including wind speed and direction, humidity, air temperature).

5. CONCLUSIONS

Substances present in the atmosphere have an impact on human health and environmental safety. At the same time air pollution can spread anywhere and cannot be limited to a selected area. Especially all kinds of uncontrolled emissions of hazardous gases (such as ammonia) can create critical situations.

Based on the analyses, the authors identified the need for applying virtual reality in combination with modelling, simulation of impurities migration and the use of UAS in detecting hazardous gas leaks. It is worth noting that the purpose of application of UAS and simulation by ALOHA is twofold: to create procedures or recommended practices of using drones, as well as to provide reliable data for simulation in real-time.

Firstly, the use of simulation allows not only a safe (because it is carried out in virtual reality) testing of scenarios, but also a development of the tactics of using UAS as well as the rules of observation and measurement. The simulation results may be helpful to determine a number of drone flight parameters (with sensors attached), which include but are not limited to:

- recommended flight altitude depending on the type of released substance,
- safe distance from the substance cloud,
- speed at which the drone should move to "keep up" with the cloud.

Thus, knowing the distribution of the substance in the cloud and its size, the operator will know how close they may fly. Moreover, by specifying the distance, the operator will be able to select a camera to the desired resolution and zoom. In that

way, thanks to simulation in a virtual reality, it is possible to create appropriate procedures, recommended practices, and finally drone flight rules for the purposes of monitoring the movement of a cloud of a dangerous substance. Additionally, the possibility of using eyes to control the drone allows to ensure the pilot's safety.

The presented concept justifies the need to develop comprehensive automated systems that would allow to simulate the leakage area in 3D and at the same time allow for the determination of UAV flight routes taking into account the direction and strength of the wind, humidity and air temperature. This could help to develop a flight path that corresponds as much as possible to the actual area of the leak and gas movement.

ACKNOWLEDGEMENTS

This research was co-funded by the National Centre for Research and Development as part of the project entitled "Controlling an autonomous drone using goggles (monocular)", no. DOB-BIO9/26/04/2018.

REFERENCES

- Abbaslou H., Karimi A., 2019. Modeling of ammonia emission in the petrochemical industry. *Jundishapur J. Health Sci.*, 11, e94101. DOI: [10.5812/jjhs.94101](https://doi.org/10.5812/jjhs.94101).
- AIRBEAM project, 2012–2015. AIRBorne information for emergency situation awareness and monitoring. Seventh framework programme of the European Community for research and technological development and demonstration activities (2007–2013). Available at: <https://cordis.europa.eu/project/id/261769>.
- Al Fayed F., Hammoudeh M., Adebisi B., Abdul Sattar K.N., 2019. Assessing the effectiveness of flying ad hoc networks for international border surveillance. *Int. J. Distrib. Sens. Netw.*, 15. DOI: [10.1177/1550147719860406](https://doi.org/10.1177/1550147719860406).
- Argasiński J.K., Lipp N., Duźmańska-Misiarczyk N., Lesicki Ł., Strojny P., 2019. The use of VR simulators for training the UAV operators and support crew, In: Feltynowski M. (Ed.), *Wykorzystanie bezzałogowych platform powietrznych w operacjach na rzecz bezpieczeństwa publicznego*. Wydawnictwo CNBOP-PIB, Józefów, 139–151. DOI: [10.17381/2019.1](https://doi.org/10.17381/2019.1).
- Bai Z., Dong Y., Wang Z., Zhu T., 2006. Emission of ammonia from indoor concrete wall and assessment of human exposure. *Environ. Int.*, 32, 303–311. DOI: [10.1016/j.envint.2005.06.002](https://doi.org/10.1016/j.envint.2005.06.002).
- Batstone D.J., Puyol D., Flores-Alsina X., Rodríguez J., 2015. Mathematical modelling of anaerobic digestion processes: applications and future needs. *Rev. Environ. Sci. Bio/Technol.*, 14, 595–613. DOI: [10.1007/s11157-015-9376-4](https://doi.org/10.1007/s11157-015-9376-4).
- Battye W., Aneja V.P., Roelle P.A., 2003. Evaluation and improvement of ammonia emissions inventories. *Atmos. Environ.*, 37, 3873–3883. DOI: [10.1016/S1352-2310\(03\)00343-1](https://doi.org/10.1016/S1352-2310(03)00343-1).
- Bein D., Bein W., Karki A., Madan B.B., 2015. Optimizing border patrol operations using unmanned aerial vehicles. *12th International Conference on Information Technology – New Generations*, 13–15.04.2015. Las Vegas, NV, USA., 479–484. DOI: [10.1109/itng.2015.83](https://doi.org/10.1109/itng.2015.83).
- Bessagnet B., Menut L., Lapere R., Couvidat F., Jaffrezo J.-L., Mailler S., Favez O., Pennel R., Siour G., 2020. High resolution chemistry transport modeling with the on-line CHIMERE-WRF model over the French Alps—Analysis of a feedback of surface particulate matter concentrations on mountain meteorology. *Atmosphere*, 11, 565. DOI: [10.3390/atmos11060565](https://doi.org/10.3390/atmos11060565).
- Bhattacharya R., Kumar G., 2015. Consequence analysis for simulation of hazardous chemicals release using ALOHA software. *Int. J. ChemTech Res.*, 8, 2038–2046.
- Bittman S., Jones K., Vingarzan R., Hunta D.E., Sheppard S.C., Tait J., So R., Zhao J., 2015. Weekly agricultural emissions and ambient concentrations of ammonia: validation of an emission inventory. *Atmos. Environ.*, 113, 108–117. DOI: [10.1016/j.atmosenv.2015.04.038](https://doi.org/10.1016/j.atmosenv.2015.04.038).
- Burgués J., Marco S., 2020. Environmental chemical sensing using small drones: a review. *Sci. Total Environ.*, 748, 141172. DOI: [10.1016/j.scitotenv.2020.141172](https://doi.org/10.1016/j.scitotenv.2020.141172).
- CAMELOT project, 2017–2021. C2 advanced multi-domain environment and live observation technologies. Horizon 2020 – the Framework Programme for Research and Innovation (2014–2020). Available at: <https://cordis.europa.eu/project/id/740736>.
- CAMEO® Software Suite. ALOHA® Example Scenarios. 2016. National Oceanic and Atmospheric Administration, U.S. Environmental Protection Agency. Available at: https://response.restoration.noaa.gov/sites/default/files/ALOHA_Examples.pdf.
- COMPASS2020 project, 2019–2021. Coordination of maritime assets for persistent and systematic surveillance. Horizon 2020 – the Framework Programme for Research and Innovation (2014–2020). <https://cordis.europa.eu/project/id/833650> (accessed on 17 February 2023).
- EPA, 2024. Acute exposure guideline levels for airborne chemicals. Available at: <https://www.epa.gov/aegl>.
- Everts S., Davenport M., 2016. Drones detect threats such as chemical weapons, volcanic eruptions. *Chemical Engineering News.*, 94(9), 36–37. Available at: <https://cen.acs.org/articles/94/i9/Drones-detect-threats-chemical-weapons.html>.
- Feltynowski M., 2019. *Wykorzystanie bezzałogowych platform powietrznych w operacjach na rzecz bezpieczeństwa publicznego*. Wydawnictwo CNBOP-PIB, Józefów, 24. DOI: [10.17381/2019.1](https://doi.org/10.17381/2019.1).
- Ferlin M., Kurela M., Monge O., Castgnet C., 2019. Smart operations in ATEX RLV environment. *8th European Conference For Aeronautics And Space Sciences (EUCASS)*. 1–4 July 2019, Madrid, Spain. 1–13. DOI: [10.13009/EUCASS2019-518](https://doi.org/10.13009/EUCASS2019-518).
- Fu H., Luo Z., Hu S., 2020. A temporal-spatial analysis and future trends of ammonia emissions in China. *Sci. Total Environ.*, 731, 138897. DOI: [10.1016/j.scitotenv.2020.138897](https://doi.org/10.1016/j.scitotenv.2020.138897).
- GAZ SYSTEM, 2018. Sustainable development report 2018. Available at: <https://www.gaz-system.pl/en/for-the-media/annual-reports.html>.
- Giannakis E., Kushta J., Bruggeman A., Lelieveld J., 2019. Costs and benefits of agricultural ammonia emission abatement options for compliance with European air quality regulations. *Environ. Sci. Eur.*, 31, 93. DOI: [10.1186/s12302-019-0275-0](https://doi.org/10.1186/s12302-019-0275-0).

- Giompapa S., Farina A., Gini F., Graziano A., di Stefano R., 2007. Computer simulation of an integrated multi-sensor system for maritime border control. *2007 IEEE Radar Conference*. 17–20 April 2007, Waltham, Massachusetts, 308–313. DOI: [10.1109/radar.2007.374233](https://doi.org/10.1109/radar.2007.374233).
- Greenblatt A., Panetta K., Agaian S., 2008. Border crossing detection and tracking through localized image processing. *2008 IEEE Conference on Technologies for Homeland Security*. 12–13 May 2008. Waltham, MA, 333–338. DOI: [10.1109/ths.2008.4534473](https://doi.org/10.1109/ths.2008.4534473).
- Gupta S.G., Ghonge M.M., Jawandhiya P.M., 2013. Review of unmanned aircraft system (UAS). *IJAR CET*, 2(4), 1646–1658. DOI: [10.2139/ssrn.3451039](https://doi.org/10.2139/ssrn.3451039).
- Hanna S.R., Briggs G.A., Hosker Jr. R.P., 1982. Handbook on atmospheric diffusion. National Oceanic and Atmospheric Administration, Oak Ridge, TN (USA). Atmospheric Turbulence and Diffusion Lab., Report No. DOE/TIC-11223 ON: DE82002045. DOI: [10.2172/5591108](https://doi.org/10.2172/5591108).
- Hiemstra P., Karssenbergh D., van Dijk A., 2011. Assimilation of observations of radiation level into an atmospheric transport model: a case study with the particle filter and the ETEX tracer dataset. *Atmos. Environ.*, 45, 6149–6157. DOI: [10.1016/j.atmosenv.2011.08.024](https://doi.org/10.1016/j.atmosenv.2011.08.024).
- Jaferník H., 2019. The Safety of unmanned aerial vehicle (UAV) missions in storm and precipitation areas. *SFT*, 54, 194–204. DOI: [10.12845/sft.54.2.2019.15](https://doi.org/10.12845/sft.54.2.2019.15).
- James M., 2015. Simplified methods of using probit analysis in consequence analysis. *Process Saf. Prog.*, 34, 58–63. DOI: [10.1002/prs.11686](https://doi.org/10.1002/prs.11686).
- Jońca J., Pawnuł M., Bezyk Y., Arsen A., Sówka I., 2022. Drone-assisted monitoring of atmospheric pollution – a comprehensive review. *Sustainability*, 14, 11516. DOI: [10.3390/su141811516](https://doi.org/10.3390/su141811516).
- Jones R., Lehr W., Simecek-Beatty D., Reynolds M., 2013. *ALOHA® Areal Locations of Hazardous Atmospheres) 5.4. 4. Technical Documentation*. U.S. Dept. of Commerce, NOAA Technical Memorandum NOS OR&R 43. Seattle, WA: Emergency Response Division, NOAA.
- Kamińska D., Sapiński T., Wiak S., Tikk T., Haamer R.E., Avots E., Helmi A., Ozcinar C., Anbarjafari G., 2019. Virtual reality and its applications in education: survey. *Information*, 10, 318. DOI: [10.3390/info10100318](https://doi.org/10.3390/info10100318).
- Kinaneva D., Hristov G., Raychev J., Zahariev P., 2019. Early forest fire detection using drones and artificial intelligence. *42nd International Convention on Information and Communication Technology, Electronics and Microelectronics (MIPRO)*. 20–24 May 2019, Opatija, Croatia, 1060–1065. DOI: [10.23919/MIPRO.2019.8756696](https://doi.org/10.23919/MIPRO.2019.8756696).
- Lambey V., Prasad A.D., 2021. A review on air quality measurement using an unmanned aerial vehicle. *Water Air Soil Pollut.*, 232, 1–32. DOI: [10.1007/s11270-020-04973-5](https://doi.org/10.1007/s11270-020-04973-5).
- Lee H.E., Sohn J.-R., Byeon S.-H., Yoon S.J., Moon K.W., 2018. Alternative risk assessment for dangerous chemicals in South Korea regulation: comparing three modeling programs. *Int. J. Environ. Res. Public Health*, 15, 1600. DOI: [10.3390/ijerph15081600](https://doi.org/10.3390/ijerph15081600).
- Liu L., Xu W., Lu X., Zhong B., Guo Y., Lu X., Zhao Y., He W., Wang S., Zhang X., Liu X., Vitousek P., 2022. Exploring global changes in agricultural ammonia emissions and their contribution to nitrogen deposition since 1980. *PNAS*, 119, e2121998119. DOI: [10.1073/pnas.2121998119](https://doi.org/10.1073/pnas.2121998119).
- Luo Z., Zhang Y., Chen W., Van Damme M., Coheur P.-F., Clarisse L., 2022. Estimating global ammonia (NH₃) emissions based on IASI observations from 2008 to 2018. *Atmos. Chem. Phys.*, 22, 10375–10388. DOI: [10.5194/acp-22-10375-2022](https://doi.org/10.5194/acp-22-10375-2022).
- Malm W.C., Schichtel B.A., Barna M.G., Gebhart K.A., Rodriguez M.A., Collett Jr. J.L., Carrico C.M., Benedict K.B., Prenni A.J., Kreidenweis S.M., 2013. Aerosol species concentrations and source apportionment of ammonia at Rocky Mountain National Park. *J. Air Waste Manage. Assoc.*, 63, 1245–1263. DOI: [10.1080/10962247.2013.804466](https://doi.org/10.1080/10962247.2013.804466).
- Mustapić M., Domitrović A., Radišić T., 2021. Monitoring traffic air pollution using unmanned aerial systems, In: Petrović M., Novačko L. (Eds), *Transformation of transportation. EcoProduction*. Springer, Cham. DOI: [10.1007/978-3-030-66464-0_11](https://doi.org/10.1007/978-3-030-66464-0_11).
- Nandu V.N., Soman A.R., 2018. Consequence assessment of anhydrous ammonia release using CFD-probit analysis. *Process Saf. Prog.*, 37, 525–534. DOI: [10.1002/prs.11970](https://doi.org/10.1002/prs.11970).
- Naseem S., King A.J., 2018. Ammonia production in poultry houses can affect health of humans, birds, and the environment – techniques for its reduction during poultry production. *Environ. Sci. Pollut. Res.*, 25, 15269–15293. DOI: [10.1007/s11356-018-2018-y](https://doi.org/10.1007/s11356-018-2018-y).
- National Academies of Sciences, Engineering, and Medicine, 2016. *Acute exposure guideline levels for selected airborne chemicals: Volume 20*. Washington, DC: The National Academies Press. DOI: [10.17226/23634](https://doi.org/10.17226/23634).
- National Research Council, 2001. *Standing operating procedures for developing acute exposure guideline levels for hazardous chemicals*. The National Academies Press, Washington, DC. 2001. DOI: [10.17226/10122](https://doi.org/10.17226/10122).
- National Research Council, 2010. *Acute exposure guideline levels for selected airborne chemicals*. Volume 9. The National Academies Press, Washington, DC. DOI: [10.17226/12978](https://doi.org/10.17226/12978).
- Neghab M., Mirzaei A., Kargar Shouroki F., Jahangiri M., Zare M., Yousefinejad S., 2018. Ventilatory disorders associated with occupational inhalation exposure to nitrogen trihydride (ammonia). *Ind. Health*, 56, 427–435. DOI: [10.2486/indhealth.2018-0014](https://doi.org/10.2486/indhealth.2018-0014).
- Orozco J.L., Van Caneghem J., Hens L., González L., Lugo R., Díaz S., Pedrosa I., 2019. Assessment of an ammonia incident in the industrial area of Matanzas. *J. Cleaner Prod.*, 222, 934–941. DOI: [10.1016/j.jclepro.2019.03.024](https://doi.org/10.1016/j.jclepro.2019.03.024).
- Pan S.-Y., He K.-H., Lin K.-T., Fan C., Chang C.-T., 2022. Addressing nitrogenous gases from croplands toward low-emission agriculture. *npj Clim. Atmos. Sci.*, 5, 43. DOI: [10.1038/s41612-022-00265-3](https://doi.org/10.1038/s41612-022-00265-3).
- Pirrone N., Keating T., (Eds), 2010. *Hemispheric transport of air pollution 2010. Part B: Mercury*. Air Pollution Studies No. 18. Economic Commission for Europe Geneva. United Nations, New York and Geneva.

- Pobkrut T., Eamsa-ard T., Kerdcharoen T., 2016. Sensor drone for aerial odor mapping for agriculture and security services. *13th International Conference on Electrical Engineering/Electronics, Computer, Telecommunications and Information Technology (ECTI-CON)*. 28 June–1 July 2016. Chiang Mai, Thailand. DOI: [10.1109/ecticon.2016.7561340](https://doi.org/10.1109/ecticon.2016.7561340).
- Rabajczyk A., Zboina J., Zielecka M., Fellner R., 2020. Monitoring of selected CBRN threats in the air in industrial areas with the use of unmanned aerial vehicles. *Atmosphere*, 11, 1373. DOI: [10.3390/atmos11121373](https://doi.org/10.3390/atmos11121373).
- Rasheed T., Bilal M., Nabeel F., Adeel M., Iqbal H.M.N., 2019. Environmentally-related contaminants of high concern: potential sources and analytical modalities for detection, quantification, and treatment. *Environ. Int.*, 122, 52–66. DOI: [10.1016/j.envint.2018.11.038](https://doi.org/10.1016/j.envint.2018.11.038).
- Sapek A., 2013. Ammonia emissions from non-agricultural sources. *Polish J. Environ. Stud.* 22, 63–70.
- Šmídl V., Hofman R., 2013. Tracking of atmospheric release of pollution using unmanned aerial vehicles. *Atmos. Environ.*, 67, 425–436. DOI: [10.1016/j.atmosenv.2012.10.054](https://doi.org/10.1016/j.atmosenv.2012.10.054).
- Sommer S.G., Webb J., Hutchings N.J., 2019. New emission factors for calculation of ammonia volatilization from european livestock manure management systems. *Front. Sustain. Food Syst.*, 3, 101. DOI: [10.3389/fsufs.2019.00101](https://doi.org/10.3389/fsufs.2019.00101).
- Sutton M.A., Dragosits U., Tang Y.S., Fowler D., 2000. Ammonia emissions from non-agricultural sources in the UK. *Atmos. Environ.*, 34, 855–869. DOI: [10.1016/S1352-2310\(99\)00362-3](https://doi.org/10.1016/S1352-2310(99)00362-3).
- Thyker-Nielsen S., Deme S., Mikkelsen T., 1999. Description of the Atmospheric Dispersion Module RIMPUFF. RODOS(WG2)-TN(98)-02. Risø National Laboratory. Available at: <https://citeseerx.ist.psu.edu/document?repid=rep1&type=pdf&doi=f41efa614a5fa79c5a7aafcdba64a284987b7fe7>.
- Tseng J.M., Su T.S., Kuo C.Y., 2012. Consequence evaluation of toxic chemical releases by ALOHA. *Procedia Eng.*, 45, 384–389. DOI: [10.1016/j.proeng.2012.08.175](https://doi.org/10.1016/j.proeng.2012.08.175).
- U.S. Department of Energy, National Nuclear Security Administration, 2007. Atmospheric dispersion model validation in low wind conditions. Final Report. DOE/NV/25946–277.
- U.S. Department of Energy, Office of Environment, Safety and Health, 2004. ALOHA computer code application guidance for documented safety analysis. Final Report. DOE-EH-4.2.1.3-ALOHA Code Guidance.
- UNECE. 1999. Protocol to abate acidification eutrophication and ground-level ozone. Available at: <https://unece.org/environment-policy/air/protocol-abate-acidification-eutrophication-and-ground-level-ozone>.
- United Nations, 2013. Protocol to the 1979 Convention on long-range transboundary air pollution to abate acidification, eutrophication and ground-level ozone. Gothenburg (Sweden), 30 November 1999. Adoption of an amendment of the text of and Annexes II to IX to the protocol and addition of new Annexes X And XI.. Available at: <https://treaties.un.org/doc/Publication/CN/2013/CN.155.2013-Eng.pdf>.
- Van Damme M., Clarisse L., Franco B., Sutton M.A., Erisman J.W., Kruit R.W., van Zanten M., Whitburn S., Hadji-Lazaro J., Hurtmans D., Clerbaux C., Coheur P.-F., 2021. Global, regional and national trends of atmospheric ammonia derived from a decadal (2008–2018) satellite record. *Environ. Res. Lett.*, 16, 055017. DOI: [10.1088/1748-9326/abd5e0](https://doi.org/10.1088/1748-9326/abd5e0).
- Van Damme M., Clarisse L., Whitburn S., Hadji-Lazaro J., Hurtmans D., Clerbaux C., Coheur P.-F., 2018. Industrial and agricultural ammonia point sources exposed. *Nature*, 564, 99–103. DOI: [10.1038/s41586-018-0747-1](https://doi.org/10.1038/s41586-018-0747-1).
- Vidi N., 2019. Drones and robots helped save Notre Dame, Available at: <https://dronebelow.com/2019/04/19/drones-and-robots-helped-save-notre-dame/>.
- Wu C., Wang G., Li J., Li J., Cao C., Ge S., Xie Y., Chen J., Liu S., Du W., Zhao Z., Cao F., 2020. Non-agricultural sources dominate the atmospheric NH₃ in Xi'an, a megacity in the semi-arid region of China. *Sci. Total Environ.*, 722, 137756. DOI: [10.1016/j.scitotenv.2020.137756](https://doi.org/10.1016/j.scitotenv.2020.137756).
- Wu Y., Gu B., Erisman J.W., Reis S., Fang Y., Lu X., Zhang X., 2016. PM_{2.5} pollution is substantially affected by ammonia emissions in China. *Environ. Pollut.*, 218, 86–94. DOI: [10.1016/j.envpol.2016.08.027](https://doi.org/10.1016/j.envpol.2016.08.027).
- Wyer K.E., Kelleghan D.B., Blanes-Vidal V., Schaubberger G., Curran T.P., 2022. Ammonia emissions from agriculture and their contribution to fine particulate matter: a review of implications for human health. *J. Environ. Manage.*, 323, 116285. DOI: [10.1016/j.jenvman.2022.116285](https://doi.org/10.1016/j.jenvman.2022.116285).
- Xiang T.-Z., Xia G.-S., Zhang L., 2019. Mini-unmanned aerial vehicle-based remote sensing: techniques, applications, and prospects. *IEEE Geosci. Remote Sens. Mag.*, 7, 29–63. DOI: [10.1109/mgrs.2019.2918840](https://doi.org/10.1109/mgrs.2019.2918840).
- Zappa C.J., Brown S.M., Laxague N.J.M., Dhakal T., Harris R.A., Farber A.M., Subramaniam A., 2020. Using ship-deployed high-endurance unmanned aerial vehicles for the study of ocean surface and atmospheric boundary layer processes. *Front. Mar. Sci.*, 6, 777. DOI: [10.3389/fmars.2019.00777](https://doi.org/10.3389/fmars.2019.00777).
- Zhan X., Adalibieke W., Cui X., Winiwarter W., Reis S., Zhang L., Bai Z., Wang Q., Huang W., Zhou F., 2021. Improved estimates of ammonia emissions from global croplands. *Environ. Sci. Technol.*, 55, 1329–1338. DOI: [10.1021/acs.est.0c05149](https://doi.org/10.1021/acs.est.0c05149).
- Zheng J., Ma Y., Chen M., Zhang Q., Wang L., Khalizov A.F., Yao L., Wang Z., Wang X., Chen L., 2015. Measurement of atmospheric amines and ammonia using the high resolution time-of-flight chemical ionization mass spectrometry. *Atmos. Environ.*, 102, 249–259. DOI: [10.1016/j.atmosenv.2014.12.002](https://doi.org/10.1016/j.atmosenv.2014.12.002).